

## Assessment of Photocatalytic Process Using Composite Photocatalysts for COD Reduction for Al-Dewaniyah Petroleum Refinery Wastewater: RSM Approach

Amani Al-Aessim  
University of Al-Qadisiyah

Husham Al -Temmimi  
University of Al-Qadisiyah

**Abstract:** A slurry bubble photoreactor with air blowing for circulating and oxidizing using composite photonanocatalyst nanoparticles ( $TiO_2/ZnO$ ) with UV radiation light lamp was used successfully to remove of COD from petroleum refinery wastewater. Effect of the main effective parameters like catalyst dosage, pH and time on the reduction efficiency (RE%) was investigated and optimized using response surface methodology (RSM). Results showed that catalyst dosage has the most significance effect on RE% with a contribution of 13.23%, followed by time with a contribution of 7.68%, and finally pH with 0.6%. The optimum results were  $TiO_2$  dosage of 1.25g/l, pH=9, and time of 103 min in which RE% of 80.7% was achieved with requiring a specific energy consumption of 25.5 kWh/m<sup>3</sup>.

**Keywords:** Petroleum refinery wastewater,  $TiO_2$  ,  $ZnO$ , $SnO_2$ , AOPs, Photocatalysis process.

### Introduction

It is commonly known that wastewater produced by the petroleum refinery industry contains high levels of organic pollutants that are harmful to both humans and the environment. Due to the high amount of fresh water used in the refinery stages of crude oil processing, they are often released in large volumes ( Haruna et al., 2022). Nations where the crude oil was refined, this is a common problem. Both organic and inorganic compounds make up the wastewater produced by petroleum refineries. For instance, heavy metals are among the inorganic substances ,nitrogen and phosphorus compounds, whereas the organic compounds that are present in large quantities in these wastewaters can be divided into three classes. The first class comprises paraffins, such as propane, ethane, and methane. The second contains naphthenes, such as cyclohexane and dimethyl cyclopentane, while the third contains aromatics, such as xylene, toluene, and benzene. As a result, these wastewaters are regarded as hazardous pollutants for the environment, and it is required that they be treated before being released into the environment(Lawan et al., 2023). Since many persistent pollutants are still present in the treated wastewaters, a significant percentage of the methods used to treat such wastewaters are deemed unsuitable, which can result in secondary pollution impacts on the environment(Lawan et al., 2023; Javadi et al., 2023; Khan et al.,2015 Alattar et al., 2023).

Numerous methods of treating wastewater have been used, including membrane filtration, adsorption, bioconversion, and reverse osmosis. All of these techniques either generated secondary pollutants or took longer to treat (Javadi et al., 2023; Khan et al., 2015; Alattar et al., 2023; Hussain et al., 2020). This is based on a comprehensive analysis of significant developments in the field of the undoped, doped or ternary  $TiO_2-SnO_2/TiO_2-ZnO/TiO_2-ZnO$  heterostructures employed as photocatalysts for the detoxification of different water contaminants. Also, the photocatalytic performances of the catalysts ,photocatalysts are dependent on essential

- This is an Open Access article distributed under the terms of the Creative Commons Attribution-Noncommercial 4.0 Unported License, permitting all non-commercial use, distribution, and reproduction in any medium, provided the original work is properly cited.

- Selection and peer-review under responsibility of the Organizing Committee of the Conference

parameters such as structure, morphology and surface area. Additionally, the impact of different factors such as pollutant concentrations catalyst loading, pH, irradiation sources on photocatalytic performance has been discussed.

Several previous studies have reported the enhanced oxidation of contaminants by the TiO<sub>2</sub>/ZnO photo-catalyst process. The photo-catalysis was used to treat petroleum wastewater and removal of 93% of phenols was achieved(Liwsirisaeng et al., 2012). Successfully degraded the benzene–toluene–xylene in refinery wastewater by using ZnO and TiO<sub>2</sub> combined with tin oxide (SnO<sub>2</sub>) to 73%, while Anju et al. (2019),enhanced the removal of phenol from 37% using ZnO/TiO<sub>2</sub> to 46% when used in combination with hydrogen peroxide (H<sub>2</sub>O<sub>2</sub>) and ZnO/TiO<sub>2</sub> process( Devipriya & Yesodharan, 2010) showed that mixing ZnO and TiO<sub>2</sub> did not produce any synergic or inhibitive effect on the catalyst and the catalyst system was improved under ultraviolet (UV) solar radiation. Ansoff (1987), achieved 30% removal of total organic carbon (TOC) by using UV/TiO<sub>2</sub> and UV/ZnO processes in a contaminated aqueous solution. Zott et al. (2011) showed that the maximum degradation of chemical oxygen demand (COD) was 36.5% and 39% after 120 min photo-catalytic of ZnO and the photo-catalytic of TiO<sub>2</sub>, respectively. Mohabansi et al. (2011),reported that the maximum degradation efficiency of methylene using TiO<sub>2</sub> and ZnO powder as a photo-catalyst under UV radiation was 99% in aqueous solutions at pH 2.

Based on the literature, the photo-catalyst of TiO<sub>2</sub> and ZnO processes has effective oxidation in wastewater treatment. However, its effectiveness in petroleum wastewater treatment is still not sufficient because of the complexity of petroleum wastewater, and an improvement for the performance of oxidation processes is required. Consequently, the combination of TiO<sub>2</sub> and ZnO can increase the production of hydroxyl radicals and improve the oxidation potential of petroleum components and wastewater.

The classical optimization technique of changing one variable at a time to study the effects of variables on the response is time consuming and cost expensive, particularly for multivariable systems, and it does not represent an effect of interactions between different factors. While statistical design of experiments is used to optimize the parameters in multivariable systems, it is a technique for obtaining significant models of a phenomenon by a minimum number of experiments and it also considers interactions among the variables( Montgomery & Montgomery, 1997; Mohajeri et al., 2015).Recently, this statistical technique has been successfully applied in many fields(Mustafa et al., 2021; Zahed & Brown, 1986 Dasgupta, 2021;Ahmad et al., 2014). The most common design under response surface methodology (RSM) is Box Behnkin design (BBD) which is efficient and flexible, providing sufficient data on the effects of variables and overall experiment error with a minimum number of experiments (Öztürk et al., 2021).

## Methods and Materials

### Characteristics of Petroleum Refinery Effluents

Table 1. Characteristics of Al-Diwaniya refinery plant wastewater

Characteristic	Outlet	Unit
pH	7	
Temperature	16	°C
TDS	14338	Ppm
BOD	20	ppm
COD	950	ppm
Phenol	32	ppm
Oil content	22.6	mg/L
Turbidity	202	NTU
PO <sub>4</sub> <sup>3-</sup>	0.129	ppm
Cl <sup>-</sup>	3050	ppm

### Chemicals

Tin Dioxide (SnO<sub>2</sub>) Nano-particles (purity 99.5%, APS 35–55 nm) was used as a photo-catalyst purchased from (NANOSHELL LLC, USA),, titanium dioxide (TiO<sub>2</sub>) nano-particles was used as a photo-catalyst purchased from ((purity 99.7 %% THOMAS BAKER, India),, Zinc Oxide (ZnO) was used as a photo-catalyst purchased from (purity 99.9 %%-- TEDIA COMPANY, INC)

## The Photocatalytic System

Figure 1 depicts the photoreactor used in this work. It is composed of a 1 L photoreactor tank that is 110 mm in diameter by 150 mm in length and is composed of Perspex. A recirculation pump (GRANDFAR: X15GR-10) was used for circulating the solution externally across the vessel with controlling its flow rate via a flow meter having a flow rate interval from 0.5 to 7 L/min. An air compressor (HAILEA ACO-318) was used for providing air to the mixture with controlling its flow rate using an air flow meter(0–5L/min)

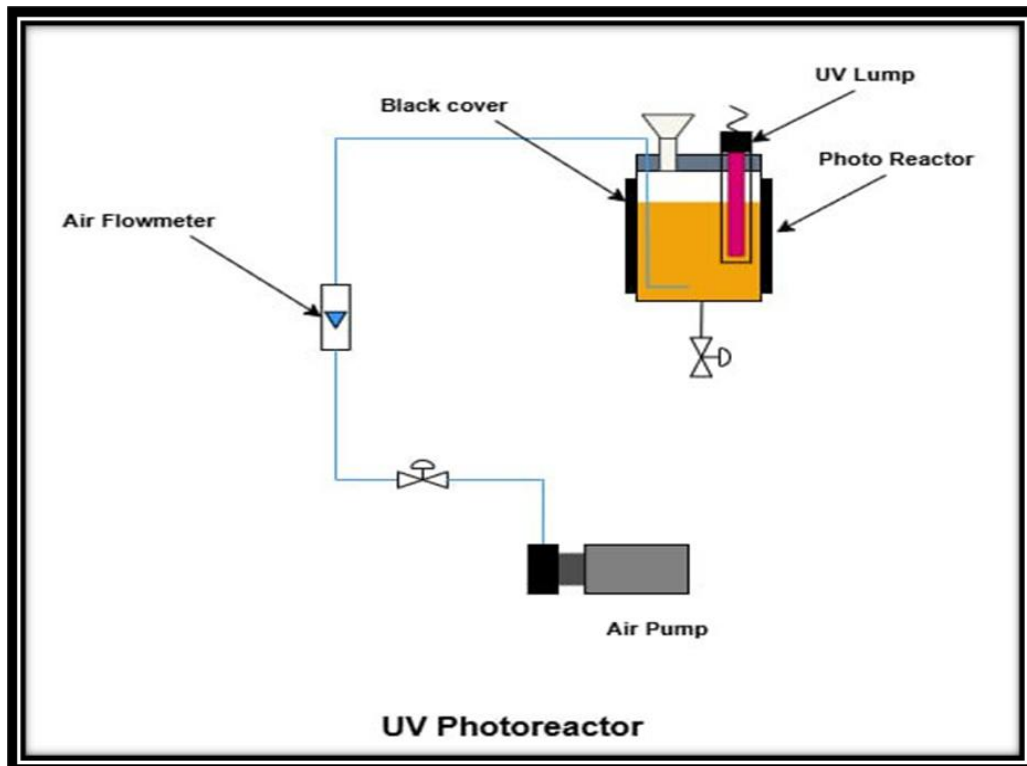


Figure 1. Photocatalytic system

One UV lump house can be inserted into each of the two 10 mm-diameter holes in the photoreactor cover. The UV lamp, which was purchased from Sterilight R-CAN (Texas, USA), was UVC (253.7 nm, 6-W, rated life 10,000 hrs.). It was placed inside two quartz tubes and completely submerged within the reactor to maximize light utilization(Ramteke & Gogate, 2016). The comparison of UVA, UVB, and UVC for degrading methylene blue as a complex organic material by (Joseph et al., 2015; Joseph et al., 2016)served as the basis for the selection of UVC in this work. It was found that only UVC could completely degrade methylene blue in 14 minutes. In addition, numerous studies have demonstrated the effectiveness of UVC in degrading different types of wastewater, such as refinery-type wastewater by TiO<sub>2</sub> ( Devipriya & Yesodharan, 2010; De Oliveira et al., 2020; Zarei et al., 2010; Mortazavian et al., 2019). and others by SnO<sub>2</sub> (Mendoza-Damián et al., 2016; Mortazavian et al., 2019; Tammina & Mandal, 2016; Diallo et al., 2016).

By feeding the effluent at the reactor's top and discharging at its bottom, directly below the UV lamp, the pump, which was positioned beneath the photoreactor, created an appropriate circulating flow that allowed the nanoparticles along the UV lamp houses to be well-mixed and suspended. Every run was carried out with a fixed liquid flow rate of 4L/min. The reactor was fed air at a steady flow rate of 3 L/min( Fan et al., 2019).By stopping electron-hole pairs from recombining, air bubbling through an air distributor was utilized to sustain the catalyst's photocatalytic activity (Haritha et al., 2016).

After bringing the pH to the necessary starting point, each run began by first combining the necessary quantity of the photocatalyst with 0.5 L of the wastewater in a 1L beaker and leaving it in the dark for 90 minutes. A funnel that was attached to the photoreactor's cover was then used to pour the effluent inside. After circulating the effluent around the reactor while supplying air at the necessary flowrate, the UV-lump were turned on, and the operation was initiated for a duration. A sample was taken to measure the COD value after the solution was filtered to remove the catalyst at the conclusion of each run. The same process was used for the kinetic study, but multiple samples were taken at 60-minute intervals throughout the operation. The batch run also followed

the same protocol, but there was no effluent circulation. In this instance, the air distributor at the reactor's bottom was the only way to mix the mixture. After that, the air pump was switched to a flow rate of 3 L/min, and samples were taken from the batch reactor every 60 minutes.

## Characterizations and Analytical Methods

### Characterization of Photocatalysts (TiO<sub>2</sub>)

The crystalline phase of TiO<sub>2</sub> particles was analysed by XRD using X-ray thin film diffractometer (XRD 6000/Shimadzu/Japan) with CuK $\alpha$  radiation of 1.5405 Å and testing 2 $\theta$  at the range 20–80°. The scan step time was 1.2 s with a step size of 0.2°. The XRD was operated at 40 kV and 30 mA. The morphology and microstructure of SnO<sub>2</sub> nanoparticles were examined by SEM FEI\_ Company, Netherlands, Inspect S50 (Model)combined with EDS with the following operating conditions: The measurement parameters were: HV = 20 kV, bias = 1400 V, bias = 0, spot = 3.0. EDX was measured via XFlash\_6110/Model, Bruker Company/Germany.

## Analytical Measurements

A popular and accurate technique for figuring out the wastewater's organic content is the chemical oxygen demand (COD) test. The test makes it possible to measure waste using the total amount of oxygen required to convert organic materials into carbon dioxide and water. The feasibility of the combined (UV/TiO<sub>2</sub>) process for the degradation of organic contaminants in wastewater from petroleum refineries was assessed in this study using COD as a response. To determine the COD value, 2 milliliters of wastewater were digested in a thermal reactor (RD125, Lovibond) using K<sub>2</sub>Cr<sub>2</sub>O<sub>7</sub> as an oxidizing agent for 120 minutes at 150 °C.

A spectrophotometer (MD200, Lovibond) was used to measure the COD concentration after the digested sample had been allowed to reach room temperature. A digital pH meter (ISOLAB Laborgerger GmbH, Germany) was used to measure the solution's pH, and a conductivity tester (HANNA Instrument Inc., Romania) was used to measure the solution's conductivity. The Hach Company/Hach Lange GmbH (USA) method 8047 was used to measure the concentration of phenol, and the Photo Flex Series (WTW, model no. 14541, Germany) was used to measure the concentration of chloride ions.

## Performance Evaluation

COD removal efficiency was calculated by Eq.(1) (Al-Tameemi et al., 2024):

$$RE\% = \frac{COD_i - COD_f}{COD_i} \times 100 \quad (1)$$

Where, RE% means COD removal efficiency, the initial value of COD in (mg/L) denotes by COD<sub>i</sub> while final value of COD in (mg/L) terms as COD<sub>f</sub>.

In this work, electrical energy consumption in the photo-catalyst process (EEC) was calculated by Eq.(1) based on the proposal of the Photochemistry Commission of the International Union of Pure and Applied Chemistry (IUPAC) as follows (El-Ghenemy et al., 2012).

$$EEC = \frac{P \times t \times 1000}{V \times \log \left( \frac{COD_i}{COD_f} \right)} \quad (2)$$

Where P is the rated power (kW) of the UV lamp, V is the volume of the solution (L), t is the reaction time (h). So, the electrical energy required for photo-catalyst process is in kWh/m<sup>3</sup>.

## Experimental Design

The traditional approach to optimizing a multi-variable system is to consider one factor at a time. This approach does not take into account the alternative effects among process variables. Additionally, it took a lot of time (Reza et al., 2017) Response surface methodology (RSM) is a set of statistical and mathematical methods used to optimize the operational conditions of the process response affected by various operating variables. The Box–Behnken design (BBD), which consists of three levels and three factors, was one of the most effective experimental designs utilized in the RSM to validate and examine the process variables that impact the removal of COD Within the BBD. The RE% was considered as a response to three process variables, which were TiO<sub>2</sub> dosage (X1), pH (X2), and time (X3). 0 (middle or central point), 1 (high level), and -1 (low level) were the codes assigned to the process variables (Vatanparast & Taghizadeh, 2016). Table 2 displays the process factors and their intended levels.

Table 2. Process parameters in the refinery wastewater treatment (coded and real levels).

Process parameters	Range in Box-Behnken		
Coded levels	Low (-1)	Middle (0)	High (+1)
X1: catalyst dosage (g/L)	0.25	0.75	1.25
X2: pH	3	6	9
X3: Time (min)	30	90	150

For obtaining the appropriate quadratic model with the acceptable statistical conditions, Box–Behnken offers the designs that required though using a portion of the selected runs for a three-level factorial. The following equation can be used to estimate the number of runs (N) required to complete a Box–Behnken design.

$$N = \gamma k (k - 1) + cp \quad (3)$$

Where k: denotes the number of process variables and cp: denotes the central point's repeated number. Based on Eq. (3.3), fifteen runs were achieved for estimating the impacts of the process factors on the RE%. Table 3.3 shows the BBD that has been suggested for this study. Depending on BBD, a second order polynomial model can be used, with the following equation describing how the interaction terms fit with the experimental results (Cui et al., 2019).

$$Y = a_0 + \sum a_i x_i + \sum a_{ii} x_i^2 + \sum a_{ij} x_i x_j \quad (4)$$

Which Y acts the response (RE), (i) and (j) denotes the index numbers for patterns,  $a_0$  : intercept term,  $x_1, x_2, \dots, x_k$  are the process factors.  $a_i$  : the 1<sup>st</sup>.order main effect,  $a_{ii}$  : the 2<sup>nd</sup>. order main effect and  $a_{ij}$  acts the influence of interaction. The regression coefficient ( $R^2$ ) was evaluated after the inferential analysis to check that the model fit was appropriate.

## Results and Discussion

### Characterizations of TiO<sub>2</sub>

Figure 2 shows the XRD pattern for nanoparticle TiO<sub>2</sub>. The 2θ at peaks 26.6°; 33.85°; 37.95°, 38.95°, 51.75°, 54.75°, 57.8°, 61.9° and 64.75°, and 65.95° corresponding to crystal indices of (110), (101), (200), (111), (211), (220), (002), (310), (112), and (301) confirm the strong diffraction peaks of TiO<sub>2</sub>. These diffraction peaks correspond to a reference line pattern (JCPDS: 41-1445) of crystalline titanium dioxide with tetragonal rutile structure (Mendoza-Damián et al., 2016). No other diffraction peaks belong to crystalline byproducts were observed. Similar observations were found by previous works (Mortazavian et al., 2019; Mendoza-Damián et al., 2016; Tammina & Mandal, 2016; Diallo et al., 2016; Fan et al., 2019).

Figure 3 shows SEM images of TiO<sub>2</sub> nanoparticle at two magnification 120kX and 30kX. Images showed that TiO<sub>2</sub> nanoparticles have some agglomeration tending to be semi-spherical shapes. Their surfaces were high porosity that enhanced the degradation of pollutants. In figure 3-a, it was observed that the range of particles sizes occurred between 32.58 and 60.86 nm confirming their nanoscale. BET Surface Area of TiO<sub>2</sub> was found to be equal to 29 m<sup>2</sup>/g. The average pore volume and diameter were found to be 0.1889 cm<sup>3</sup>/g ( $p/p_0=0.990$ ) and 13.302 nm, respectively. A higher number of active sites with a greater amount of light absorption were happen if a larger BET surface area was used leading to further increase the efficiency of the photo-catalytic reaction (Long et al., 2020).

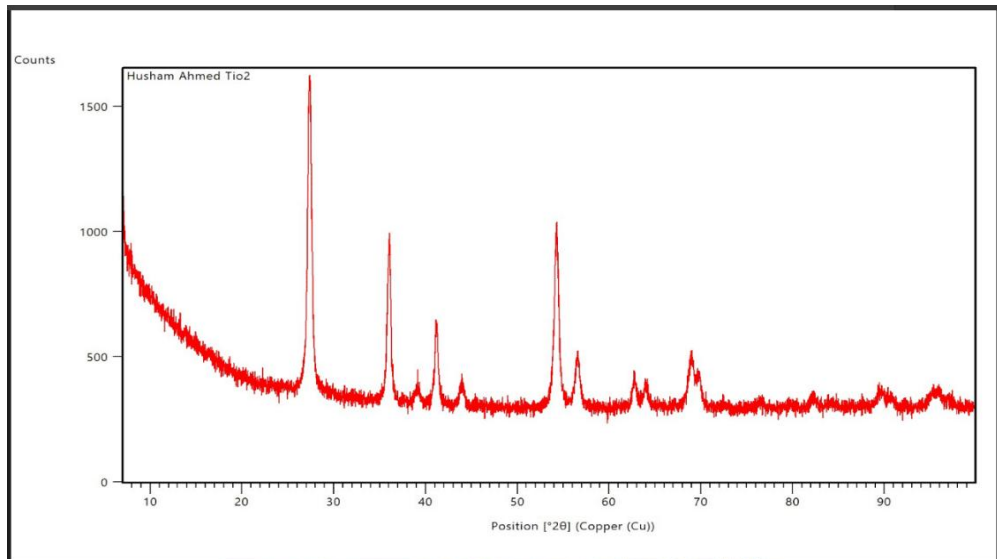
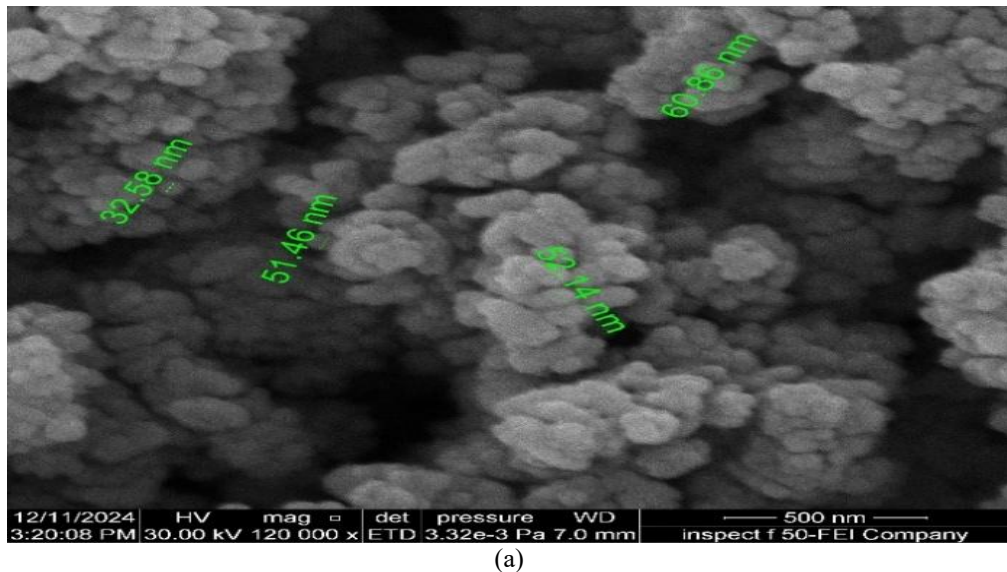
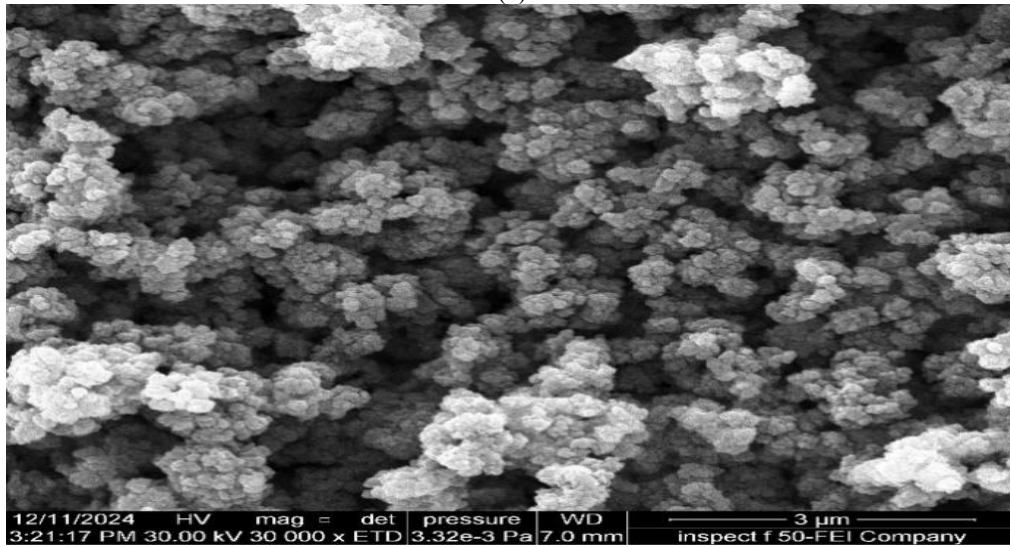


Figure 2. XRD pattern for nanoparticle  $\text{TiO}_2$



(a)



(b)

Figure 3. SEM images of  $\text{TiO}_2$  nanoparticles. a) magnification 12kX, b) magnification 30kX

## RSM Results of COD Removal by Photocatalytic Process (UV/ TiO<sub>2</sub>- ZnO)

Fifteen experiments were carried out at various sets to investigate the shared effects of the process variables on COD removal. The experimental results for RE% along with the values predicted by the model equation are shown in Table 3. Table 3 also mentions electrical energy consumption (EEC). As can be observed, EEC ranges from 8.8 to 70.579 kWh/m<sup>3</sup>, while RE% falls between 60.52 and 80.31 percent. Less than 2% of the centered point values differed, indicating that the model was highly reproducible.

Table 3. Results of COD removal by photocatalytic process (UV/ TiO<sub>2</sub>- ZnO)

Run Order	Pt Type	Blocks	TiO <sub>2</sub> dosage (g/L)	pH	Time (min)	RE%	EEC (kWh/m <sup>3</sup> )
1	2	1	1.25	9	90	80.31579	25.5
2	0	1	0.75	6	90	74.84211	30.03
3	2	1	0.25	9	90	75.05263	29.851
4	2	1	0.25	6	150	62.42105	70.579
5	2	1	1.25	3	90	79.89474	25.839
6	2	1	0.75	9	30	60.52632	14.862
7	2	1	1.25	6	30	73.05263	10.535
8	2	1	0.75	3	150	64.84211	66.08
9	0	1	0.75	6	90	64.94737	39.536
10	2	1	0.75	9	150	64.10526	67.42
11	0	1	0.75	6	90	68.63158	35.749
12	2	1	0.25	6	30	76.94737	9.4150
13	2	1	1.25	6	150	77.05263	46.928
14	2	1	0.25	3	90	72.94737	31.7018
15	2	1	0.75	3	30	78.94737	8.86642

By using Minitab-19 Software, a quadratic model based on the real values of the process factors was formulated as indicated by

$$RE\% = 65.94 - 47.83 X_1 + 0.52 X_2 + 0.2999 X_3 + 36.91 X_1 X_1 - 0.004 X_2 * X_2 - 0.001450 X_3 * X_3 - 0.281 X_1 * X_2 + 0.0043 X_1 * X_3 - 0.00044 X_2 * X_3 \quad (5)$$

Where X<sub>1</sub>, X<sub>2</sub>, X<sub>3</sub> act as process variables (TiO<sub>2</sub>) dosage, pH, and Time respectively while X<sub>1</sub>X<sub>2</sub>, X<sub>1</sub>X<sub>3</sub> and X<sub>2</sub>X<sub>3</sub> act as the interaction influence among these variables. (X<sub>1</sub>)<sup>2</sup>, (X<sub>2</sub>)<sup>2</sup> and (X<sub>3</sub>)<sup>2</sup> symbolizes a measure of the fundamental influence of the process variables. Antagonistic and synergistic effects are revealed by (+,-) signs in front of the coefficient of system variables as well as their interaction terms.

Table 4 explains the (ANOVA) data of the response model in which: DF symbolize (degree of freedom), Seq SS symbolize (sum of the square), Adj. SS symbolize (adjusted sum of the square), Adj. MS symbolize (adjusted mean of the square), and Contr. % represents the contribution for each factor. Fishers : (F-test) and (P-test) were used to check the capacity of the model where high value of Fisher means that maximum limits of diversity may be fitted by using the equation of regression. The (P-value) utilized to determine whether F has a high value that is reasonable to distinguish the statistical importance of model. 95% of the changeable of the model could be discussed when its (P-value) < 5%..

According to findings of Table 4, the quadratic model is essential with F-value of 20.20 at confidence level above 95 % (P-value equal to 0.0001). The lack of fit test may be utilized to see if the chosen model is acceptable for describing the data or if a more extensive model is required. The (P-value) for lack of fit in the current work equal to 0.1, which is larger than (0.05), demonstrating that was not statically important when compared to the pure error. As a result, the model can acquire reasonable prediction matching to the response values. The R<sup>2</sup> and adj. R<sup>2</sup> values in this research were assessed to be 0.975 and 0.92, respectively, confirming the model-predicted and experimental values' consistency.

According to Table 4 and it can be seen that catalyst dosage(TiO<sub>2</sub> dosage) (X<sub>1</sub>) was the most significance parameter effecting on the RE% with 13.23% as a percentage of contribution indicating the role of catalyst on the decomposition of organic contaminants during the photodegradation. The impact of time (X<sub>3</sub>) was in the second level with a percentage of contribution equal to 7.64% while pH(X<sub>2</sub>) has the lower impact on the RE% with a percentage of contribution equal to 0.61%. Additionally, the impact of 2-way interaction on the RE% was

very small with a contribution of 0. 14% that could be ignored hence all 2-way interactions are non-significant. The contribution of the squared terms (75.70%) is significant.

Table 4. ANOVA results of COD removal by the photocatalytic process (UV/ TiO<sub>2</sub>- ZnO)

Source	DF	Seq. SS	Contr.%	Adj. SS	Adj. MS	F-value	P-value
Model	9	572.614	97.32%	572.614	63.624	20.20	0.002
Linear	3	126.421	21.49%	126.421	42.140	13.38	0.008
X1	1	77.844	13.23%	77.844	77.844	24.71	0.004
X2	1	3.618	0.61%	3.618	3.618	1.15	0.333
X3	1	44.959	7.64%	44.959	44.959	14.27	0.013
Square	3	445.391	75.70%	445.391	148.464	47.13	0.000
X1*X1	1	344.301	58.52%	314.416	314.416	99.81	0.000
X2*X2	1	0.497	0.08%	0.005	0.005	0.00	0.971
X3*X3	1	100.593	17.10%	100.593	100.593	31.93	0.002
2-Way Inter.	3	0.802	0.14%	0.802	0.267	0.08	0.965
X1*X2	1	0.710	0.12%	0.710	0.710	0.23	0.655
X1*X3	1	0.068	0.01%	0.068	0.068	0.02	0.889
X2*X3	1	0.025	0.00%	0.025	0.025	0.01	0.933
Error	5	15.750	2.68%	15.750	3.150		
Lack of fit	3	2.051	0.35%	2.051	0.684	0.10	0.953
Pure-Error	2	13.699	2.33%	13.699	6.849		
Total	14	588.364	100.00%				
Model Summary		S	R <sup>2</sup>	R <sup>2</sup> (adj.)	Press	R <sup>2</sup> (pred.)	
		1.77484	97.32%	92.50%	63.6460	89.18%	

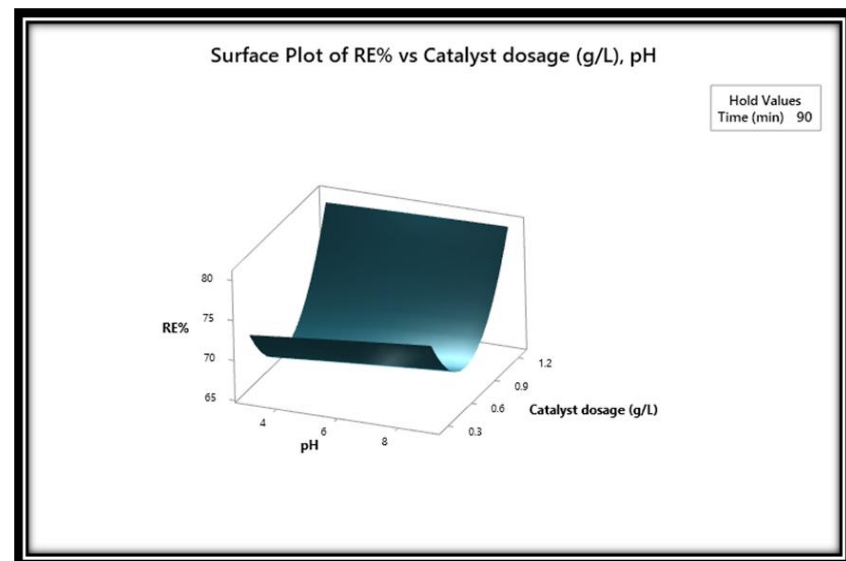
## Effect of Operating Parameters

Graphical presentation of quadratic model relied on RSM was functioned to know the influence of process variables and their combinations on the RE%. Figure (4-a, b) illustrate the combined impacts of (TiO<sub>2</sub>-ZnO dosage) and (pH) on the RE% at the middle value of time (90 min). Figure (4-a) shows the response surface plot while Figure(4-b) represents the equivalent contour sketch.

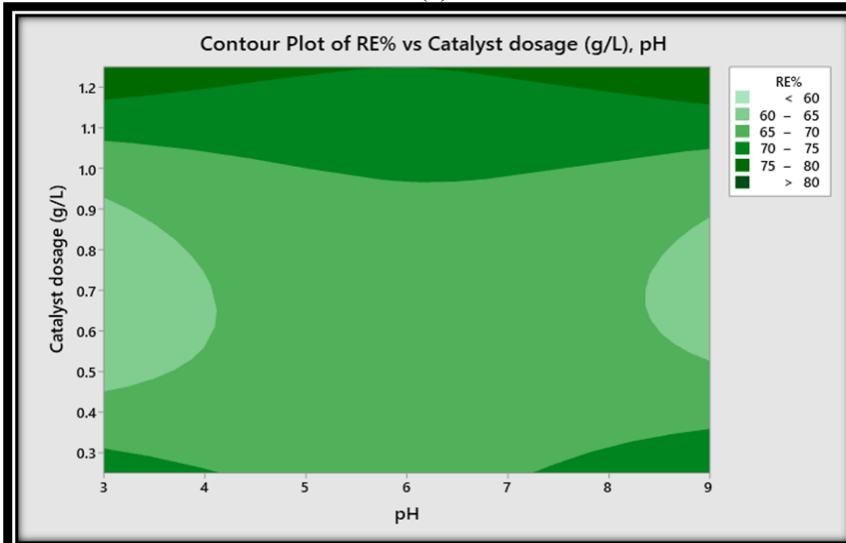
From Figure(4/a), it can be seen that RE% decrease with increasing the dosage of (TiO<sub>2</sub>-ZnO) up to 0.6 and then the RE% began to increase when the dosage of (TiO<sub>2</sub>/ZnO) increase to 1.25 leads to increase in the COD removal efficiency whereas, the behavior regarding to the impact of pH was also found on COD removal efficiency increasing slightly with increase pH value. Figure (2-b), it is obvious that R.E% >80 % might be gained within a region in which pH is (3-5, 7.3-9) and TiO<sub>2</sub>-ZnO dosages 1.15 - 1.2 g/l.

As revealed by previous works, the photocatalytic degradation rate increases with an increase in the dosage of the catalyst up to an optimum value due to increasing the surface area available for pollutant adsorption and the number of reaction sites figure (5-a) it was showed increasing in time (at 100 min) and catalyst dosage more than (1.1 g/l) and constant pH=6 leads to enhancement in RE% ,while figure(5-b) it is obvious that R.E% >80 % might be gained within a region in which time (>100min) and TiO<sub>2</sub>-ZnO dosages (<1.1 g/l). From Figure (6-a), it was cleared that an increase in the pH and the time (up to 110 min) results in an increase in the RE%, and so directly effects the pollutant removal rates. According to the contour plot results (Figure 6 /b), it is possible to get RE% >80 within a region in which time is (75–125 min) and pH is (8.5–9).

Barakat et al., 2005; Long et al., 2020; Ran et al., 2019). Also its observe the RE% increased with increasing in time values .The surface charge of TiO<sub>2</sub> is positive (Tetteh & Rathilal, 2020; Ahmed et al., 2011).unlike the alkaline medium (>5.5) where it becomes negatively charged ( Tetteh et al., 2020).However, most of the organic compounds in ORW (like SOG, phenol, and other phenolic derivatives) are negatively charged (Tetteh & Rathilal, 2020; Ahmed et al., 2011)..Hence acidic medium favors their electrostatic force of attraction towards the TiO<sub>2</sub> charged surface( Ahmed et al., 2011;Barakat et al., 2005; Long et al., 2020; Long et al., 2020; Ran et al., 2019; Liu et al.,2019). In both cases, increasing the catalyst dosage as a function of time increased their removal.

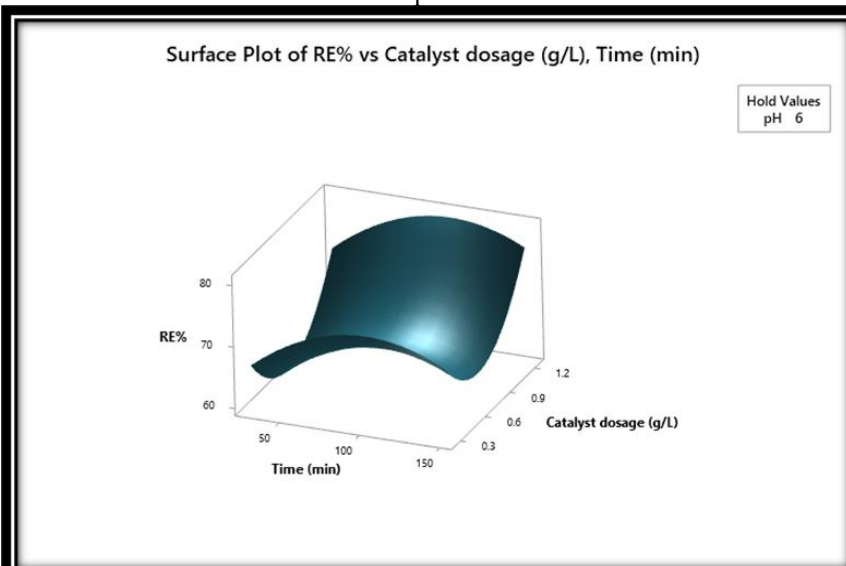


(a)

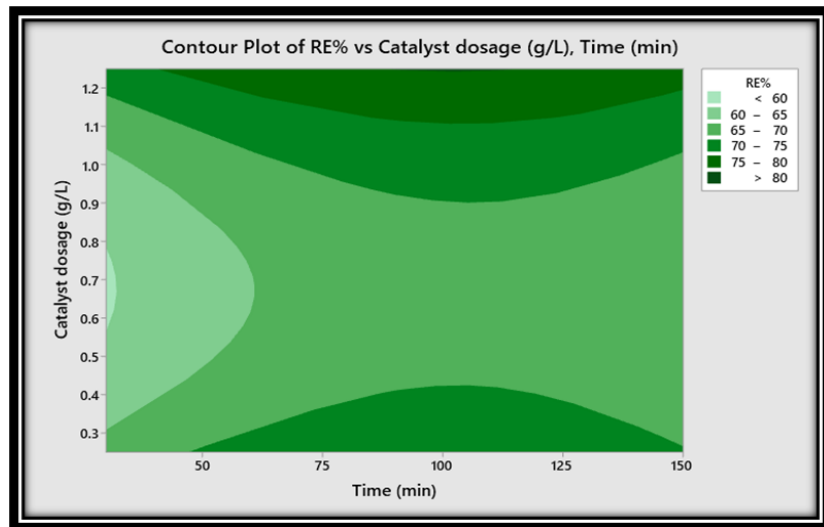


(b)

Figure 4 (a) 3D plot of interaction between catalyst dosage and pH, (b) contour plot between catalyst dosage and pH.

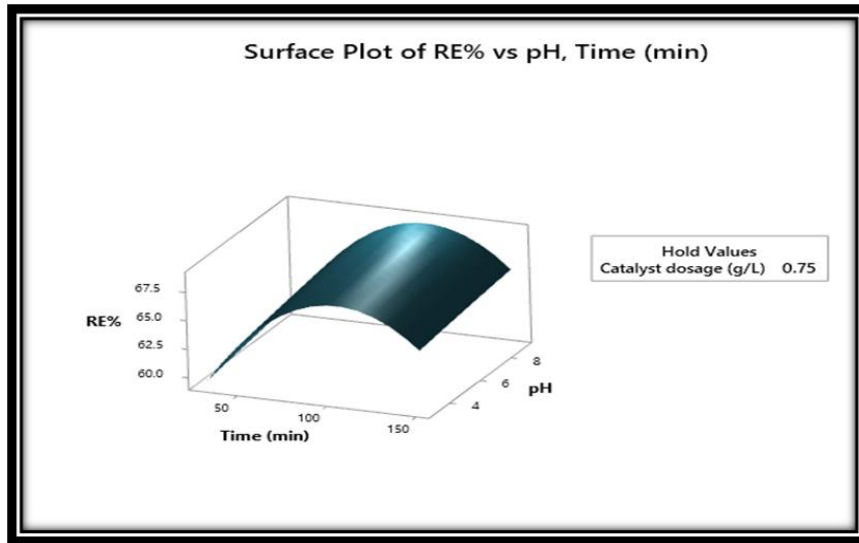


(a)

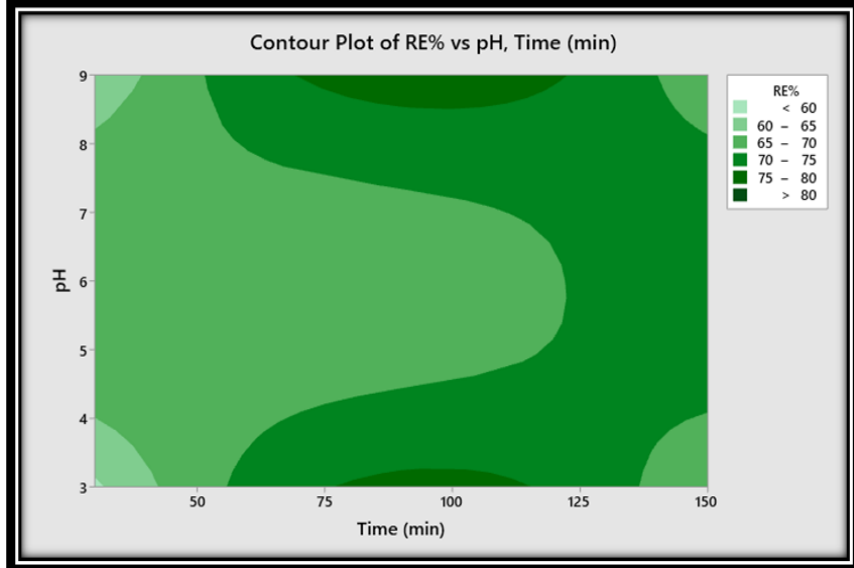


(b)

Figure 5. (a) 3D plot of interaction between catalyst dosage and time, (b) contour plot between catalyst dosage and time..



(a)



(b)

Figure 6. (a) 3D plot of interaction between pH and time, (b) contour plot between pH and time.

## Optimization

For any optimization process, the aim is to obtain the maximum value of the response with a minimum cost of energy. Consequently, RE% was nominated as the maximum, with desirability function ( $D_F$ ) of 1.0. Optimization has been determined via a response optimizer of Minitab-19 Software. Optimization results are clarified in Table 5. Results showed that the best theoretical removal of RE% is 80.70% which could be obtained at  $TiO_2$  -  $ZnO$  dosage of 1.25 g/l, pH = 9, and time of 103.939 min.

Table 5. Response optimization based on RE%

Response	Aimed	Lower	Target	Upper	Weight	Importance
RE (%)	Max.	58.94	Max	80.315	1	1
Results Parameters						
$TiO_2$ (g/L)	pH	Time (min)	RE%	$D_F$	SE	95% PI
1.25	9	103.939	80.70	1	1.56 (76.69, 84.71)	(74.63, 86.77)

## Verification of the Results

Table 6 demonstrated two experiments were carried out based on the optimized parameters for confirming the optimization results. At 103 min of the photocatalysis process, (80.7%) COD removal efficiency (average value) was achieved which is in compatible with the range of the optimum value obtained from optimal results (Table 6). Accordingly, Box-Behnken design with  $D_F$  can be functioned as effective approach features for optimizing RE% by photocatalysis process using  $TiO_2$ - $ZnO$  as catalyst.

Table 6. Confirmative runs for optimum of RE%

Run	$TiO_2$ - $ZnO$ dosage (g/l)	pH	Time (min)	$COD_F$ (ppm)	RE%	$EEC_T$ (kWh/m <sup>3</sup> )
1	1.25	9	103	187	80.7	25.5
2	1.25	9	103	180	81	24.3

Table 7. shows a comparison between the treated effluent by photocatalysis process with untreated effluent. According to Table 7, It is worth mentioning, that the treated pollutants have improve characteristics with RE% of 80.7% and final COD value of 187 ppm and achieving higher than 90% removal of turbidity.

Table 7. Comparison between the treated effluent by photocatalyst process with untreated effluent.

Characteristic	Untreated	Treated by $UV/TiO_2+ZnO$	Unit
pH	7	8.6	-
Temperature	16	28	°C
TDS	14338		Ppm
COD (ppm)	950	187	Ppm
Turbidity	113	4.3	NTU

## Conclusion

A simple photocatalytic degradation process ( $UV/TiO_2$ - $ZnO$ ) was applied successfully to treat petroleum refinery wastewater via a slurry bubble photoreactor that used both circulation and direct irradiation to degrade contaminants. Effect of operating parameters such as  $TiO_2$ - $ZnO$  dosage, pH and time was studied based on RSM. An optimal and relatively low dosage of  $TiO_2$ - $ZnO$  catalyst (1.25 g L<sup>-1</sup>) was needed with initially adjusting the solution pH at 9 to get a significant removal of COD (80.7%) during 103 min in which a specific energy consumption of 25.5 kWh/m<sup>3</sup> was required.

## Scientific Ethics Declaration

\* The authors declare that the scientific ethical and legal responsibility of this article published in EPSTEM journal belongs to the authors.

## Conflict of Interest

\* The authors declare that they have no conflicts of interest

## Funding

\* No funding.

## Acknowledgements

\* This article was presented as an oral presentation at the International Conference on Engineering and Advanced Technology (ICEAT) held in Selangor, Malaysia, on July 23-24, 2025.

\* The authors acknowledge the assistance of chemical engineering department, the University of Al-Qadisiyah.

## References

Ahmad, A. S., Hassan, M. Y., Abdullah, M. P., Rahman, H. A., Hussin, F., Abdullah, H., & Saidur, R. (2014). A review on applications of ANN and SVM for building electrical energy consumption forecasting. *Renewable and Sustainable Energy Reviews*, 33, 102–109.

Ahmed, S., Rasul, M. G., Brown, R., & Hashib, M. A. (2011). Influence of parameters on the heterogeneous photocatalytic degradation of pesticides and phenolic contaminants in wastewater: A short review. *Journal of Environmental Management*, 92(3), 311–330.

Alattar, S. A., Sukkar, K. A., & Alsaffar, M. A. (2023). Enhancement of ozonation reaction for efficient removal of phenol from wastewater using a packed bubble column reactor. *Indonesian Journal of Chemistry*, 23(2), 383–394.

Al-Tameemi, H. M., Sukkar, K. A., & Abbar, A. H. (2024). Treatment of petroleum refinery wastewater by a combination of anodic oxidation with photocatalyst process: Recent advances, affecting factors and future perspectives. *Chemical Engineering Research and Design*, 204, 487–508.

Anju, S., Ashtami, J., & Mohanan, P. V. (2019). Black phosphorus, a prospective graphene substitute for biomedical applications. *Materials Science and Engineering: C*, 97, 978–993.

Ansoff, H. I. (1987). Strategic management of technology. *Journal of Business Strategy*, 7(3), 28–39.

Barakat, M. A., Schaeffer, H., Hayes, G., & Ismat-Shah, S. (2005). Photocatalytic degradation of 2-chlorophenol by Co-doped TiO<sub>2</sub> nanoparticles. *Applied Catalysis B: Environmental*, 57(1), 23–30.

Dasgupta, S. P. (2021). *The economics of biodiversity: The Dasgupta review (abridged version)*. HM Treasury. Retrieved from <https://assets.publishing.service.gov.uk/pdf>

De Oliveira, C. P. M., Viana, M. M., & Amaral, M. C. S. (2020). Coupling photocatalytic degradation using a green TiO<sub>2</sub> catalyst to membrane bioreactor for petroleum refinery wastewater reclamation. *Journal of Water Process Engineering*, 34, 101093.

Devipriya, S. P., & Yesodharan, S. (2010). Photocatalytic degradation of phenol in water using TiO<sub>2</sub>. *Journal of Environmental Biology*, 31, 247–249.

Diallo, A., Manikandan, E., Rajendran, V., & Maaza, M. (2016). Physical & enhanced photocatalytic properties of green synthesized SnO<sub>2</sub> nanoparticles via *Aspalathus linearis*. *Journal of Alloys and Compounds*, 681, 561–570.

Dong, X. A., Cui, W., Wang, H., Li, J., Sun, Y., Wang, H., ... & Dong, F. (2019). Promoting ring-opening efficiency for suppressing toxic intermediates during photocatalytic toluene degradation via surface oxygen vacancies. *Science Bulletin*, 64(10), 669–678.

El-Ghenemy, A., Garcia-Segura, S., Rodríguez, R. M., Brillas, E., El Begrani, M. S., & Abdelouahid, B. A. (2012). Optimization of the electro-Fenton and solar photoelectro-Fenton treatments of sulfanilic acid solutions using a pre-pilot flow plant by response surface methodology. *Journal of Hazardous Materials*, 221–222, 288–297.

Fan, W., Zhou, Z., Wang, W., Huo, M., Zhang, L., Zhu, S., ... & Wang, X. (2019). Environmentally friendly approach for advanced treatment of municipal secondary effluent by integration of micro-nano bubbles and photocatalysis. *Journal of Cleaner Production*, 237, 117828.

Haritha, E., Roopan, S. M., Madhavi, G., Elango, G., Al-Dhabi, N. A., & Arasu, M. V. (2016). Green chemical approach towards the synthesis of SnO<sub>2</sub> NPs in argument with photocatalytic degradation of diazo dye and its kinetic studies. *Journal of Photochemistry and Photobiology B: Biology*, 162, 441–447.

Haruna, A., Chong, F. K., Ho, Y. C., & Merican, Z. M. A. (2022). Preparation and modification methods of defective titanium dioxide-based nanoparticles for photocatalytic wastewater treatment—a comprehensive review. *Environmental Science and Pollution Research*, 29(47), 70706–70745.

Hussain, Z., Fadhil, Z., Kareem, S., Mohammed, S., & Yousif, E. (2020, August). Removal of organic contaminants from textile wastewater by adsorption on natural biosorbent. *Materials Science Forum*, 1002, 489–497. Trans Tech Publications Ltd.

Javadi, A., Nourizade, M., Rahmani, M., & Eckert, K. (2023). Interaction of catalyst nanoparticles and pollutant molecules in photocatalytic wastewater treatment: Novel characterization via dynamic surface properties. *Chemical Engineering Science*, 269, Article 118459.

Joseph, C. G., Taufiq-Yap, Y. H., Li Puma, G., Sanmugam, K., & Quek, K. S. (2016). Photocatalytic degradation of cationic dye simulated wastewater using four radiation sources, UVA, UVB, UVC and solar lamp of identical power output. *Desalination and Water Treatment*, 57(17), 7976–7987.

Joseph, D. L., Jin, J., Newman, D. A., & O'Boyle, E. H. (2015). Why does self-reported emotional intelligence predict job performance? A meta-analytic investigation of mixed EI. *Journal of Applied Psychology*, 100(2), 298–342.

Khan, W. Z., Najeeb, I., Tuiyebayeva, M., & Makhtayeva, Z. (2015). Refinery wastewater degradation with titanium dioxide, zinc oxide, and hydrogen peroxide in a photocatalytic reactor. *Process Safety and Environmental Protection*, 94, 479–486.

Lawan, M. S., Kumar, R., Rashid, J., & Barakat, M. A. E. F. (2023). Recent advancements in the treatment of petroleum refinery wastewater. *Water*, 15(20), 3676.

Liu, H., Chen, P., Yuan, X., Zhang, Y., Huang, H., Wang, L. A., & Dong, F. (2019). Pivotal roles of artificial oxygen vacancies in enhancing photocatalytic activity and selectivity on Bi<sub>2</sub>O<sub>2</sub>CO<sub>3</sub> nanosheets. *Chinese Journal of Catalysis*, 40(5), 620–630.

Liwsirisaeng, P., Kalambaheti, C., Pongkao Kashima, D., Jemsirilert, S., & Jinawath, S. (2012). Photocatalytic degradation of phenolic compounds by TiO<sub>2</sub> powder. In *18th International Conference on Composite Materials* (pp. 1–4).

Long, D., Chen, Z., Rao, X., & Zhang, Y. (2020). Sulfur doped g-C<sub>3</sub>N<sub>4</sub> and BiPO<sub>4</sub> nanorods hybrid architectures for enhanced photocatalytic hydrogen evolution under visible light irradiation. *ACS Applied Energy Materials*, 3(1), 119–127.

Mendoza-Damián, G., Tzompantzi, F., Pérez-Hernández, R., Gómez, R., & Hernández-Gordillo, A. (2016). Photocatalytic properties of boehmite–SnO<sub>2</sub> composites for the degradation of phenol. *Catalysis Today*, 266, 82–89.

Mohabansi, N. P., Patil, V. B., & Yenkie, N. (2011). A comparative study on photo degradation of methylene blue dye effluent by advanced oxidation process by using TiO<sub>2</sub>/ZnO photocatalyst. *Rasayan Journal of Chemistry*, 4(4), 814–819.

Mohajeri, S. H., Grizzi, S., Righetti, M., Romano, G. P., & Nikora, V. (2015). The structure of gravel-bed flow with intermediate submergence: A laboratory study. *Water Resources Research*, 51(11), 9232–9255.

Montgomery, W. W., & Montgomery, S. K. (1997). Montgomery thyroplasty implant system. *The Annals of Otology, Rhinology & Laryngology*, 106(9), 1.

Mortazavian, S., Saber, A., & James, D. E. (2019). Optimization of photocatalytic degradation of acid blue 113 and acid red 88 textile dyes in a UV-C/TiO<sub>2</sub> suspension system: Application of response surface methodology (RSM). *Catalysts*, 9(4), 360.

Mustafa, A. A., Derise, M. R., Yong, W. T. L., & Rodrigues, K. F. (2021). A concise review of *Dendrocalamus asper* and related bamboos: Germplasm conservation, propagation and molecular biology. *Plants*, 10(9), 1897.

Mustafa, A. A., Derise, M. R., Yong, W. T. L., & Rodrigues, K. F. (2021). A concise review of *Dendrocalamus asper* and related bamboos: Germplasm conservation, propagation and molecular biology. *Plants*, 10(9), 1897.

Öztürk, H., Barışçı, S., & Turkay, O. (2021). Paracetamol degradation and kinetics by advanced oxidation processes (AOPs): Electro-peroxone, ozonation, goethite catalyzed electro-Fenton and electro-oxidation. *Environmental Engineering Research*, 26(2), Article e200646.

Ramteke, L. P., & Gogate, P. R. (2016). Treatment of real industrial wastewater using the combined approach of advanced oxidation followed by aerobic oxidation. *Environmental Science and Pollution Research*, 23, 9712–9729.

Ran, M., et al. (2019). Light induced generation and regeneration of oxygen vacancies in BiSbO<sub>4</sub> for sustainable visible light photocatalysis. *ACS Applied Materials & Interfaces*, 11(51), 47894–47902.

Reza, K. M., Kurny, A. S. W., & Gulshan, F. (2017). Parameters affecting the photocatalytic degradation of dyes using  $\text{TiO}_2$ : A review. *Applied Water Science*, 7, 1569–1578.

Tammina, S. K., & Mandal, B. K. (2016). Tyrosine mediated synthesis of  $\text{SnO}_2$  nanoparticles and their photocatalytic activity towards Violet 4 BSN dye. *Journal of Molecular Liquids*, 221, 415–421.

Tammina, S. K., & Mandal, B. K. (2016). Tyrosine mediated synthesis of  $\text{SnO}_2$  nanoparticles and their photocatalytic activity towards Violet 4 BSN dye. *Journal of Molecular Liquids*, 221, 415–421.

Tetteh, K. E., & Rathilal, S. (2020). Evaluating pre- and post-coagulation configuration of dissolved air flotation using response surface methodology. *Processes*, 8(4), 383.

Tetteh, K., Obotey Ezugbe, E., Rathilal, S., & Asante-Sackey, D. (2020). Removal of COD and  $\text{SO}_4^{2-}$  from oil refinery wastewater using a photo-catalytic system—Comparing  $\text{TiO}_2$  and zeolite efficiencies. *Water*, 12(1), 214.

Vatanparast, M., & Taghizadeh, M. T. (2016). One-step hydrothermal synthesis of tin dioxide nanoparticles and its photocatalytic degradation of methylene blue. *Journal of Materials Science: Materials in Electronics*, 27, 54–63.

Zahed, I., & Brown, G. E. (1986). The Skyrme model. *Physics Reports*, 142(1–2), 1–102.

Zarei, M., Khataee, A. R., Ordikhani-Seyedlar, R., & Fathinia, M. (2010). Photoelectro-Fenton combined with photocatalytic process for degradation of an azo dye using supported  $\text{TiO}_2$  nanoparticles and carbon nanotube cathode: Neural network modeling. *Electrochimica Acta*, 55(24), 7259–7265.

Zott, C., Amit, R., & Massa, L. (2011). The business model: Recent developments and future research. *Journal of Management*, 37(4), 1019–1042.

---

**Author(s) Information**

---

**Amani Al-Aessam** **Husham Al -Temmimi**  
University of Al-Qadisiyah, College of Engineering University of Al-Qadisiyah, College of Engineering  
Al-Dewaniyah, Iraq Al-Dewaniyah, Iraq  
Contact e-mail: [Amani.chem.eng@qu.edu.iq](mailto:Amani.chem.eng@qu.edu.iq)

---

**To cite this article:**

Al-Aessam, A. & Al-Temmimi, H. (2025). Assessment of photocatalytic process using composite photocatalysts for COD reduction for Al-Dewaniyah Petroleum refinery wastewater: RSM approach. *The Eurasia Proceedings of Science, Technology, Engineering and Mathematics (EPSTEM)*, 37, 37-50.